Proceedings of the 6th Nordic Signal Processing Symposium - NORSIG 2004
June 9 - 11, 2004
Espoo, Finland

Automatic Registration of Spectrophotometric Retinal Images

Gisli H. Halldorsson[1], Jon Atli Benediktson[1], Gunnar Mar Zoega[2], Thor Eysteinsson[3], and Einar Stefansson[2]

[1]University of Iceland, [2]University Hospital of Iceland and [3]University of Iceland
[1]Dept. of Electrical and Computer Engineering, [2]Dept. of Ophthalmology and [3]Dept. of Physiology
[1]P.O. Box Hjardarhagi 6, 107 Reykjavik
ICELAND
[1]Email: {ghh,benedikt}@hi.is

ABSTRACT

This study is a part of the development of a system that enables analysis of spectrophotometric measurements of oxygen saturation in the retinal vasculature. A digital fundus camera is used to capture four spectral images using an image splitter with 542 nm, 558 nm, 586 nm and 605 nm band-pass filters. Before the spectral images can be used to analyze the optical density ratios they have to go through a preprocessing stage where they are registered together in software. The registration process is different from previous registration algorithms because the images are at very low resolution and therefore we propose a more data oriented method. To validate the registration we propose a method which uses the distance between edges in images. This method could be valuable to quantify the registration accuracy in more general image registration problems.

1. INTRODUCTION

Examination of images of the fundus (back of the eye) is an important diagnostic tool in ophthalmology. Fundus images allow inspection of arteries and veins that are usually hidden beneath the skin. Consequently, fundus images may be used to diagnose many diseases that affect the vascular structure. The measurement of oxygen saturation in the retinal vasculature is known as *retinal oximetry*. Noninvasive retinal oximetry may provide vital clinical information about the metabolic state of the retina. If the total blood flow and oxygen saturations in both the retinal arterioles and veins are calculated, the difference between the oxygen delivered to and away from the retina can be examined. This information can be used to further the understanding of retinal function in health and disease [1].

This study is a part of the development of a system that enables analysis of spectrophotometric measurements of oxygen saturation in the retinal vasculature. Fundus images are taken with a digital camera through an image splitter which produces an image which contains four smaller sub-images corresponding to the wavelengths: 542 nm, 558 nm, 586 nm and 605 nm. An example of an image is shown in Fig. 1. To enable analysis of the retinal oximetry, the sub-images (here referred to as *spectral images*) must go through a preprocessing stage

542 nm 558 nm

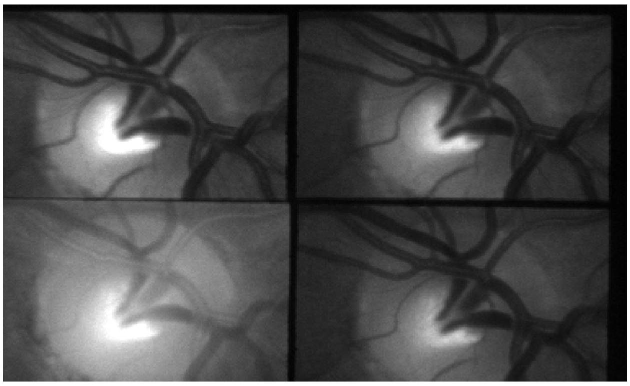

605 nm 586 nm

Fig. 1 A multispectral spectrophotometric retina image. The image contains four spectral images of the fundus which correspond to different wavelengths.

were they are registered as pairs. It is also desirable for the registration to be automatic since manual registration can be both very time consuming and inaccurate. Although image registration in general is well known in the literature [2] and retinal image registration in particular [3]–[7], the problem of spectrophotometric images has not been addressed before. The methods which have been proposed earlier did not seem to fit this problem. Therefore, we propose a more data oriented method, which is described here.

The paper is organized as follows. In Section 2, the spectrophotometric retinal images are introduced and the problem is formulated. The proposed registration method is described in Section 3. Validation of the registration is given in Section 4. Experimental results are given in Section 5. Finally, conclusions are drawn in Section 6.

2. SPECTROPHOTOMETRIC RETINAL IMAGE

The spectrophotometric retinal images were acquired using a fundus camera/microscope, which was connected to a digital camera. A schematic image of the current prototype can be seen in Fig. 2. Before the image (flash reflection) enters the solid-state camera detector, it is sent through an image splitter that splits the image into four optical paths. A narrow band-pass filter (with center wavelengths 542 nm, 558 nm, 586 nm, and 605 nm) is located in each optical path. Each path is of equal

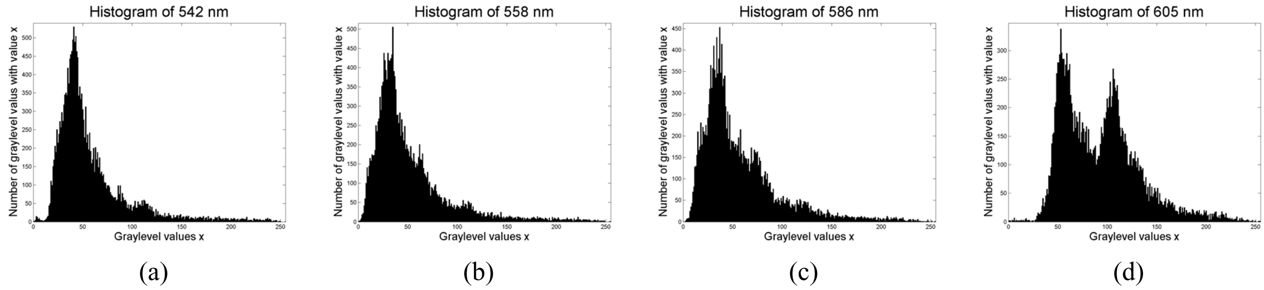

Fig. 3 Histogram of the spectral images: (a) 542 nm, (b) 558 nm, (c) 586 nm and (d) 605 nm.

length so that each image hits the sensor at the same time. To control both the path length and the displacement (position) of the sensor, a series of front surface mirrors are used. The mirrors can be moved on rails by means of a microcaliber mechanism.

Output of the digital camera is sent to a computer where the multispectral image is stored (Fig. 1 shows an output image from the system described above). The output image is a 382x255 pixel 16 bit gray scale image. The image has to go through contrast enhancement before it is manipulated. The contrast enhancing is necessary because the gray-level values in the image are very poorly distributed over the 16 bits. As can be seen in Fig. 1,

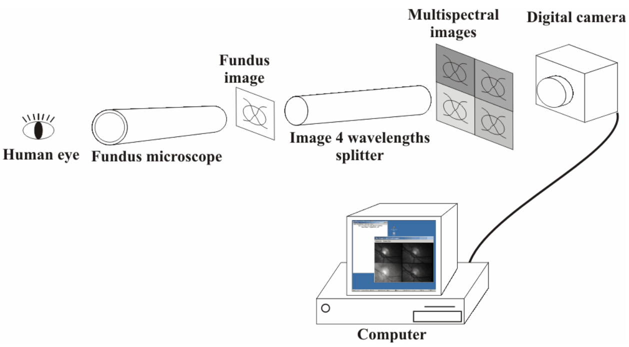

Fig. 2 Schematic image of setup to acquire spectrophotometric retinal images for the oximetry analysis.

the multispectral image consists of four spectral images. Each image is about 180×120 pixels in size. Because of mechanical sensitivity, an accurate spectral image position and rotation on the original image is not known[1]. For this reason, the images can overlap and sometimes parts of the spectral images do not hit the multispectral image (are out side of the multispectral image).

Obviously, each spectral image represents the same area of the retina but does not have the same distribution of gray-level values. Fig. 3 shows a the histogram for the spectral images in Fig. 1 after contrast enhancement and transformation to 8 bit gray-level values [0,. . .,255]. The 605 nm image appears to be dissimilar to the other spectral images because absorption of light in the retinal is smaller in this wavelength. This caused some problems in the registration, mainly for two reasons:

1) Some of the vessels in the image seem to vanish. That could cause problems if we would like to use vessels and branch points as landmarks in the registration process as in [3]–[5].
2) The optic disk is both brighter and larger in the 605 nm image than in the other images. That eliminates the possibility of using the center of the optic disk to find the image position because its apparent increase in size is not uniform in all directions.

Although the content of the spectral images is not always the same, we should be able to use the border of the spectral images in the registration process. Their borders are relatively static objects because each spectral image has at least one visible border on the original image and the border shape is almost a straight line that is easily detected using a standard edge detection algorithm.

2.1 Formulation of the Problem

The purpose of the proposed algorithm is to automatically register the four spectral images, in order to be able to process them in the same coordinate system. Recall that the mechanical sensitivity of the device to capture the images does only produce uncertainty in the image position (translation) and orientation (rotation). After examining large amount of data we concluded that the uncertainty is no more than ±20 pixels in the horizontal and vertical directions. And the uncertainty in spectral image orientation is no more than ±10°. Therefore, for each pair of images that we need to register, the first one is defined as input image $I_{\text{input}}(x, y)$ and the other is defined as reference image $I_{\text{ref}}(x, y)$. Then, the objective is to find a spatial transformation T that transforms the input image into the coordinate system of the reference image.

$$I_{\text{ref}}(x, y) = I_{\text{input}}(T(x, y)) \tag{1}$$

To find this transformation we need search for the best transformation given a search space of possible transformations. The search space here is composed of 2-D rotations $\theta \in [-10° : \Delta\theta : 10°]$ and translations $(t_x, t_y) \in [-20 : \Delta t : 20]$ pixels, the step size was configured to be $\Delta\theta = 0.5°$ and $\Delta t = 1$ pixel.

$$T_{\theta,t_x,t_y} : \begin{bmatrix} x_1 \\ y_1 \end{bmatrix} \rightarrow \begin{bmatrix} x_2 \\ y_2 \end{bmatrix} \iff$$

$$\begin{bmatrix} x_2 \\ y_2 \end{bmatrix} = \begin{bmatrix} t_x \\ t_y \end{bmatrix} + \begin{bmatrix} \cos\theta & -\sin\theta \\ \sin\theta & \cos\theta \end{bmatrix} \begin{bmatrix} x_1 \\ y_1 \end{bmatrix} \tag{2}$$

[1]Thermal changes in the room can cause a small changes in mirror position which can lead to changes in spectral image position.

To quantify what is the best transformation we need to define a similarity metric C to measure the closeness of fit between the images in the same coordinate system. The similarity metric uses the intensity values from the overlapping portion of the reference image and the transformed input image to calculate the goodness of particular transformation. The registration problem can then be formulated as to find a set of transformation-parameters $\{\tilde{\theta}, \tilde{t}_x, \tilde{t}_y\}$ that maximizes the similarity between the images, or

$$\{\tilde{\theta}, \tilde{t}_x, \tilde{t}_y\} = \underset{\theta, t_x, t_y}{\arg\max} \left[C(I_{\text{ref}}(x, y), I_{\text{input}}(T_{\theta, t_x, t_y}(x, y))\right] . \quad (3)$$

3. THE REGISTRATION ALGORITHM

The explored strategy is to split the registration algorithm into two steps. First, we estimate the orientation of each image and, then, we find the translation.

3.1 Estimation of the Orientation

The orientation of the image can be estimated without using the similarity metric, because each spectral image has at least one visible border on the multispecral image. First, the borders of the spectral images were extracted using the Canny edge detection algorithm [8]. The binary edge image in Fig. 4 was obtained by edge detecting the image in Fig. 1 using the Canny algorithm. By using an edge map we could extract horizontal and vertical borders of each spectral image. Although the spectral images lie close together or overlap we can discriminate between their borders using the gradient direction of the edge. The extracted borders are stored as binary images, which are then transformed using the Hough transformation [9]. The Hough transformation is used to find how many points lie on lines that have orientation in a particular range. Therefore, we can estimate the orientations of the spectral images' borders by choosing the line that intersects the maximum number of points. Finally, the orientation of each spectral image is calculated using a weighted average of the border orientation, weighting each possible border with how many points the border line intersects.

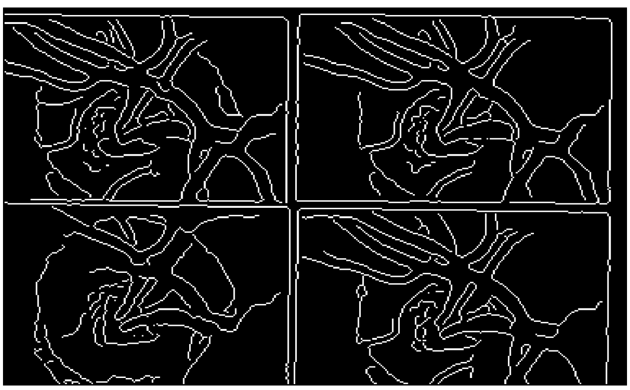

Fig. 4 Binary image of an edge map obtained by edge detecting the image on Fig. 1 and thresholding the edge map.

3.2 Estimation of the Translation

After the images have been rotated for orientation equalization, the translation between them is evaluated. First, we redefine the registration problem by

$$\{\tilde{t}_x, \tilde{t}_y\} = \underset{t_x, t_y}{\arg\max} \left[C(I_{\text{ref}}(x, y), I_{\text{input}}(T_{t_x, t_y}(x, y))\right] . \quad (4)$$

To search for the best translation, we propose an edge based similarity metric. The metric uses the attributes of edges found using the Canny edge detection on both images. The metric is given by

$$C(t_x, t_y) = \sum_{E_{\text{ref}}} \sum_{E_{\text{input}}} M(E_{\text{ref}}(x, y), E_{\text{input}}(x - t_x, y - t_y)) \quad (5)$$

where E_{ref} and E_{input} are edges from the overlapping portion of the images I_{ref} and I_{input}, respectively, (t_x, t_y) is the translation between the images. M is a binary function $M(E_{\text{ref}}(x, y), E_{\text{input}}(i, j)) \in \{0, 1\}$ and is equal to one, if the edges E_{ref} and E_{input} have the same coordinates in the reference coordinate system ($(x, y) = (i, j)$) and have a similar gradient orientation (±45°).
For a number of reasons the edges seem to be a good option in this case. Edges represent much of the intrinsic structures of these low resolution spectral images. Also, the gradient orientation of edges is an important feature to discriminate between two close edges which for example belong to different sides of a vessel. And, moreover, because this similarity metric is only used to detect the translation, the edge detection is only performed ones at the begin of the search (it is not necessary to detect the edges for each translation) because the edges are preserved while translating the images. Therefore, we only have to find which of the edges are in the overlapping portion of the images. That is an advantage since the edge detection algorithm can be computationally demanding.

4. VALIDATION OF THE REGISTRATION ALGORITHM

We used two methods to evaluate the registration error. First, a visual evaluation using a fused edge map based on the registered images. After the images have been registered as pairs we compose a fused edge map containing the edges from both images. Edges from both images which are exactly aligned, or in other words, have the same coordinates are colored white. Other edges that do not have a corresponding edge are colored in distinct gray-level values corresponding to the image which the came from. Such a map can be seen in Fig. 5, the map was used to evaluate the registration of two spectral images from Fig. 1. Using this map we can evaluate the registration error by observing gray lines with distinct gray-level values lie side by side.
In [4] the registration error was evaluated by extracting

the retina vessel centerline from the registered images and for each point on the centerline: the distance to the nearest centerline point was found in the second image. The median of these distances is taken as registration error. Median statistics are used to discard error measures from either missing or spurious centerlines. Our second method to evaluate the registration error is based on this method. However, instead of using the centerline we use the distances between edges. We prefer edges instead of centerline because centerlines can be hard to detect for these low resolution images and moreover, the edges are the core of our registration algorithm and therefore, we find it appropriate to use them in order to evaluate the registration. As said before, edges do often represent most of the intrinsic structures of images and therefore, this method could be useful to evaluate registration accuracy in more general registration problems (where retinal images are not involve).

Table 1 Estimated registration accuracy (mean±standard deviation) pixels. Using visual estimation (Visual) and median distance between edges (Edge Dist.)

	542nm/558nm	542nm/586nm	542nm/605nm	Overall
Visual	0.62±0.52	0.88± 0.42	1.00±0.38	0.83±0.47
Edge Dist.	0.69±0.48	1.09± 0.69	1.18±0.33	0.99±0.56

5. EXPERIMENTS

The visual evaluation and edge distance methods were used to evaluate registration of 50 multispectral images (150 registration problems), which were registered using the proposed registration algorithm. Table 1 summarizes the mean evaluated registration error for registration problems where the 542 nm spectral image was used as an reference image and 558 nm, 586 nm and 605 nm spectral images were used as input images.

Both evaluation methods are consistent, showing that the mean overall registration accuracy is $\leq$1 pixel. The accuracy of the algorithm is better than we hoped for because the translation step size Δt was set to one pixel in the algorithm configuration and we did not expect to get sub-pixel accuracy.

The visual evaluation method is valuable for verification of the registration algorithm, but the method requires expertise to quantify the registration accuracy, thus, the visual method alone could not be used validate the registration. The median edge distance method shows to be very consistent with the visual method and therefore, to be valuable in quantifying the registration accuracy. Although we state that our method quantifies the registration error, we cannot with absolute certainty, quantify local registration errors. However, given that we can transfer error measurement obtained by reference, we can eventually say that it is unlikely for the error to exceed a certain bound [10].

6. CONCLUSION

A registration algorithm to register multispectral retinal images was proposed. The retinal images are of very low resolution and are, therefore, not suitable for other registration algorithms (for example [4], [5]). Our proposed method is more data oriented and uses the borders of the images to evaluate the orientation and edge based similarity metric to evaluate the translation between images. The registration algorithm is fully automatic and is shown to be accurate. To validate the registration we propose a method which uses the distance between edges in images. This method could be valuable to quantify the registration accuracy for more general image registration problems.

Fig. 5 Example of a fused edge map, which is used for the visual evaluation of the registration. This particular edge map is a fusion of edge maps based on 542 nm and 558 nm spectral images, their edge maps are shown in Fig.4. In this case we can see that the white pixels are distributed all over the map and, thus, the registration error is zero.

REFERENCES

[1] A.Harris, R. B. Dinn, L. Kagemann, and E. Rechtman, “A review of methods for Human Retinal Oximetry,” *Ophthalmic Surgery, Lasers and Imaging*, vol. 34, no. 2, pp. 152–164, 2003.

[2] L. Brown, “A survey of images registration techniques,” *ACM Comput. Surv.*, vol. 24, no. 4, 1992.

[3] G.K. Matsopoulos, N.A. Mouravliansky, K.K. Delibasis, and K.S. Nikita, “Automatic Retinal Image Registration Scheme Using Global Optimization Techniques,” *IEEE Transactions on Information in Biomedicine*, vol. 3, no. 1, pp. 47–60, 1999.

[4] A. Can, C.V. Stewart, B. Roysam, and H.L. Tanenbaum, “A Feature-Based, Robust, Hierarchical Algorithm for Registering Pairs of Images of the Curved Human Retina,” *IEEE Transactions on Pattern Analysis and Machine Intelligence*, vol. 24, no. 3, pp. 347–364, March 2002.

[5] F. Lalibert, L. Gagnon, and Y. Sheng, “Registration and Fusion of Retinal Images-An Evaluation Study,” *IEEE Transactions on Medical Imaging*, vol. 22, no. 5, pp. 661–673, 2003.

[6] N. Ritter, R. Owens, J. Cooper, R.H. Eikelboom, and P.P. van Saarloos “Registration of Stereo and Temporal Images of the Retina,” *IEEE Transactions on Medical Imaging*, vol. 18, no. 5, pp. 404–418, 1999.

[7] F. Zana and J.C. Klein, “A Multimodal Registration Algorithm of Eye Fundus Images Using Vessels Detection and Hough Transform,” *IEEE Transactions on Medical Imaging*, vol. 18, no. 5, pp. 419–428, 1999.

[8] J. Canny, “A Computational Approach to Edge Detection,” *IEEE Transactions on Pattern Analysis and Machine Intelligence*, vol. 8, no. 6, pp. 679–698, 1986.

[9] P. V. C. Hough, “Methods and Means for Recognizing Complex Patterns,” U.S. Patent 3069654, 1962.

[10] J. B. Antoine Maintz and Max A. Viergever, “A survey of medical image registration,” *Medical Image Analysis*, vol. 2, no 1, pp. 1–36, 1998.